Proceedings World Geothermal Congress 2010
Bali, Indonesia, 25-29 April 2010

Application of Thermal Remote Sensing for Geothermal Mapping, Lake Naivasha, Kenya

Michael S. Pastor

Geothermal and Coal Resources Development Division,

Energy Resource Development Bureau

Department of Energy

Energy Center, Merritt Road, Fort Bonifacio,

Taguig City, Philippines

mikepastor68@yahoo.com / mpastor@doe.gov.ph

Keywords: remote sensing, thermal images, Lake Naivasha

ABSTRACT

Remote sensing of the earth's surface records energy reflected or radiated by an object at different wavelengths of the electromagnetic spectrum. The wavelength region of 3-14 μm is called thermal infrared region. The Landsat Thematic Mapper (TM) band 6 usually referred to as the thermal band operates in the wavelength of 10.4-12.5 μm with ground resolution of 120 meters. The tone of a thermal image expresses surface radiant temperature. Radiation emitted by the ground objects is measured for temperature estimates.

Lake Naivasha, a freshwater lake, and the geothermal areas surrounding it lie on the central part of the Kenya Rift Valley (KRV). Its water is being used not only for domestic water supply and agriculture but also for the exploitation of geothermal energy. Surface manifestations, in the form of hot springs, fumaroles, solfatara, altered grounds and other volcanic-related features that are common in geothermal areas are present in Lake Naivasha and are indications of the presence of geothermal resource at depth.

A qualitative and quantitative interpretation of the thermal image south of Lake Naivasha shows that thermal manifestations and structural features in general show a relation with high heat flow. Geothermal manifestations including the wells show up on the image as scattered points with high temperature pixels with values ranging from 20-40 ^{o}C. They appear to be restricted on the west side of the main thermal divide in a NE-SW direction especially along the Olkaria Fault Zone that cuts through the geothermal area.

1. INTRODUCTION

Remotely sensed data has been widely used as an exploration tool for mineral, petroleum and geothermal development as well as environmental assessment. The use of remotely sensed images gives synoptic view of large areas in lesser time.

Thermal images have been used to determine thermal characteristics of volcanoes, delineate areas of steaming and altered grounds and hot spring activities, determine rock types and locate geologic faults/fractures. The tone of a thermal image expresses surface radiant temperature. Cooler areas appear darker and warmer areas light. The radiant temperature of a given object depends on many thermal factors, such as emissivity, conductivity, capacity, diffusivity and inertia. Because of these factors, different materials warm and cool at different rates during the day and night.

A thermal image requires more insight and care in interpretation. In thermal infrared (IR) sensing, radiation emitted by the ground objects is measured for temperature estimates.

The use of thermal image was applied for a geothermal area south of Lake Naivasha, Kenya. A raw grey tone image of Landsat TM band 6 south of Lake Naivasha, which was acquired February 2000 courtesy of ITC, was used in the study.

This paper will show the application of thermal images for geothermal mapping. The objective of which is to verify the relationship between thermal anomalies to geothermal features, rock types and geologic structures.

The use of thermal images in geothermal exploration and assessment hopefully would provide a better picture of the geothermal areas and help identify the most promising site for more extensive exploration efforts.

2. BACKGROUND

Remote Sensing of the earth's surface records energy reflected or radiated by an object at different wavelengths of the electromagnetic spectrum. When EM energy is incident on any given earth surface features, it can either be reflected, absorbed and/or transmitted. The proportions of energy reflected, absorbed and transmitted will vary for different earth features, depending on their material type and condition and will also vary at different wavelengths.

The wavelength region of 3-14 μm is called thermal infrared region (Figure 1). Beyond about 4 μm in the EM spectrum energy from the Earth's surface is majorly due to radiant emission from natural materials. Any object having a temperature greater than absolute zero emits radiation whose intensity and spectral composition are a function of the material type involved and the temperature of the object under consideration. The Landsat TM band 6 usually referred to as the thermal band operates in the wavelength 10.4-12.5 μm with ground resolution of 120 meters.

The variations in tone or Digital Number (DN) in a thermal image are measures of radiant emission of the surface and not reflectance.

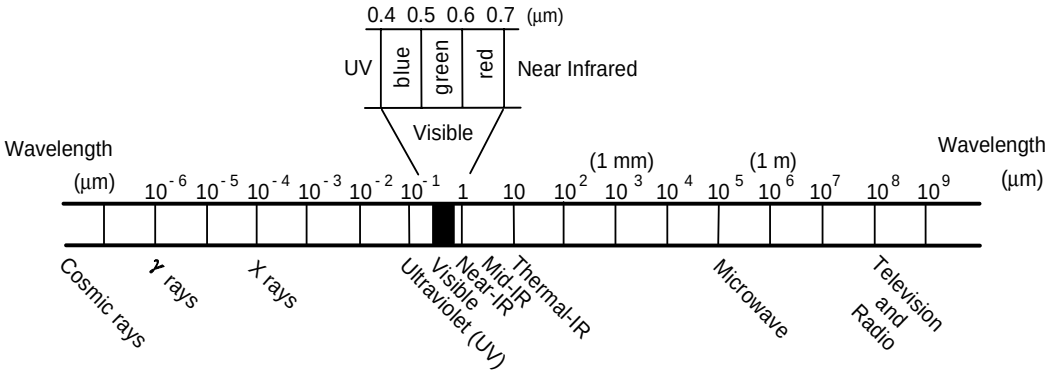


Figure 1: EM Spectrum

3. DESCRIPTION OF AREA

3.1 Location

Lake Naivasha and the geothermal areas surrounding it lie on the central part of the Kenya Rift Valley (KRV). Olkaria Geothermal Area owned by the Kenya Power Company is located south of Lake Naivasha (Figure 2). It is the only high temperature geothermal system in Africa that is used to generate electricity with an installed capacity. The Olkaria geothermal system is located within the central sector of the Kenya Rift Valley, where it is associated with a region of Quaternary volcanism.

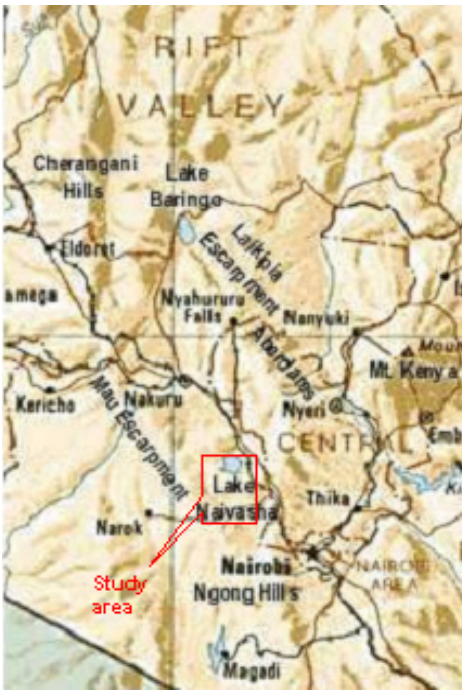


Figure 2: Location Map of Lake Naivasha

3.2 Physiography

Lake Naivasha is the highest of the rift valley lakes. It is about 1885 meters above sea level with a mean depth of 4.9 meters. The study area, which is south of the lake, is characterized by various volcanic landforms. On the southeast side of the lake is Longonot Volcano while on the southwest side is the Greater Olkaria Volcanic Complex.

Longonot Volcano occupies an area of approximately 350 km^2 and attains a maximum elevation of 2,776 masl. Arcuate lava flow fronts form distinct topographic features on its northern, eastern and southern slopes. Unlike Longonot Volcano, the Greater Olkaria Volcanic Complex is composed of several volcanic centers. Most occur as either steep sided domes or as thick lava flows of restricted lateral extent (Clarke, et. al,. 1990)

3.3 Geology

The KRV is mostly underlain by volcanics with phonolitic, trachytic and rhyolitic composition and their sedimentary derivatives. The KRV volcanics were erupted nearly continuously from Early Miocene to Holocene times.Late Tertiary and Quaternary Volcanics, lacustrine sediments and alluvium principally of reworked volcanic debris underlie the area (Figure 3). Most are volcanic rocks that include alkali rhyolites, ashes, pumiceous deposits and trachytes. Lacustrine deposits occur mostly close to the lake.

The southeast part of the area is mainly covered with pyroclastic deposits and lava flows coming from Longonot Volcano. The pyroclastics include ashes, tuff and pumiceous deposits. Lava flow is predominantly of trachytic composition.

The southwest part referred to as the Olkaria Volcanic Complex is also covered with volcanic rocks and lacustrine sediments. Most are volcanic rocks that include alkali rhyolites, ashes, pumiceous deposits and trachytes. The main products of volcanism in the area have been alkali rhyolite and pyroclastic rocks while trachyte and basalts have been minor products. The volcanic centers are structurally controlled and most of the flows are erupted through fault zones. The most recent volcanism is associated with the Ololbutot rhyolite flow. A large fraction of the pyroclastic deposits originated from Longonot Volcano.

The structural pattern in the study area trends in a N-S, NW-SE, NNW-SSE and ENE-WSW direction. Faults and fractures are more common in the in the western part (Olkaria Volcanic Zone) including the Olkaria geothermal area compared to the eastern part (Longonot Volcano) where large volumes of pyroclastic deposits are present. The younger N-S faults and fractures are common in the axial region of the rift and represent the latest tectonic activity. Verticaly permeability along some of these faults is indicated by the occurrence of strong fumarolic activity. The NW-SE trending faults are mostly inferred from aerial photos and the alignment of volcanic centers. The ENE-SSE trending faults called Olkaria Fault Zone cuts through the geothermal area and are the most important permeable structure in the whole Olkaria Geothermal Area. Thermal manifestations include fumaroles, altered grounds and hot springs.

4. INTERPRETATION

4.1 Qualitative Interpretation

A qualitative interpretation of the TM-6 image of the area shown in Figure 4 validated by limited ground checks show the following salient features:

- Several NW-SE trending parallel to sub-parallel thermal divides that coincide with structural features that are present in the area. The most distinct of these, considered as the main thermal divide, coincides with the Gorge Farm Lineament. The N-S trending Ololbutot Fault does not show well in the image perhaps because of the agricultural area on the surface, which blocks out this signature.

- A generally lighter tone on the Mt. Longonot slopes compared to the generally dark tone on the Olkaria Volcanic Zone that is separated by the Gorge Farm Lineament. The contrast in tones is due to the difference in lithology. The Mt. Longonot Area is underlain mostly of pyroclastic materials consisting of ash and pumice while the OVC is mostly covered with volcanic rocks consisting of alkali rhyolites, pyroclastic deposits and trachytes. A highly porous rock such as pumice displays rapid diurnal variations in temperature because of its low thermal inertia and thus appears lighter in the image. Thermal inertia is a measure of the resistance of a material to change its temperature in response to a change in the temperature of its surroundings. A material with low thermal inertia heats up quickly to a high temperature during the day and cools in a similar fashion.

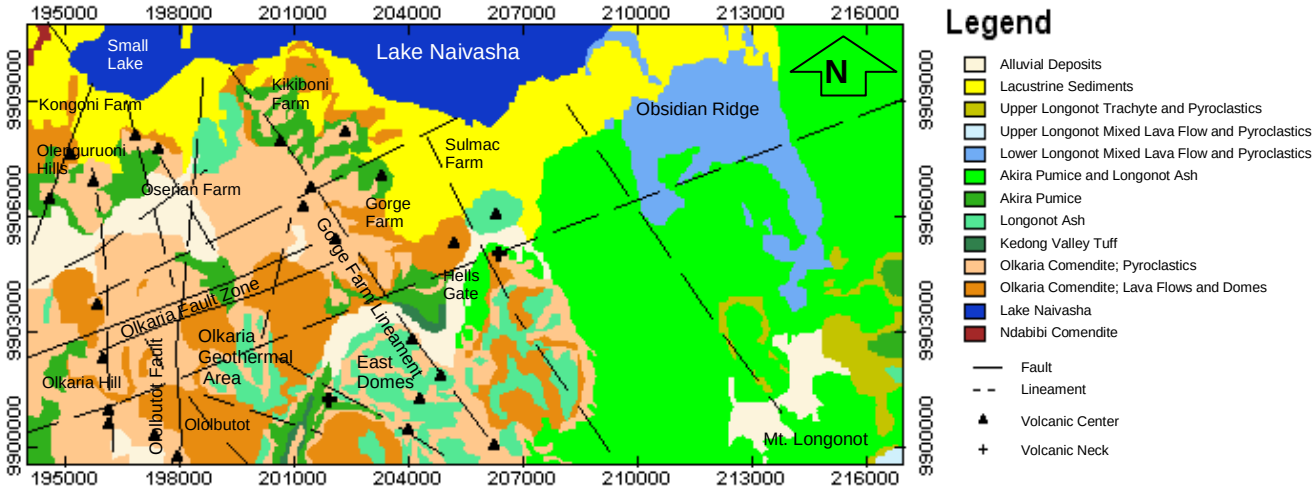


Figure 3: Simplified Geologic Map Lake Naivasha, Kenya (Adapted from Clarke, M. C. G. et. al. 1990

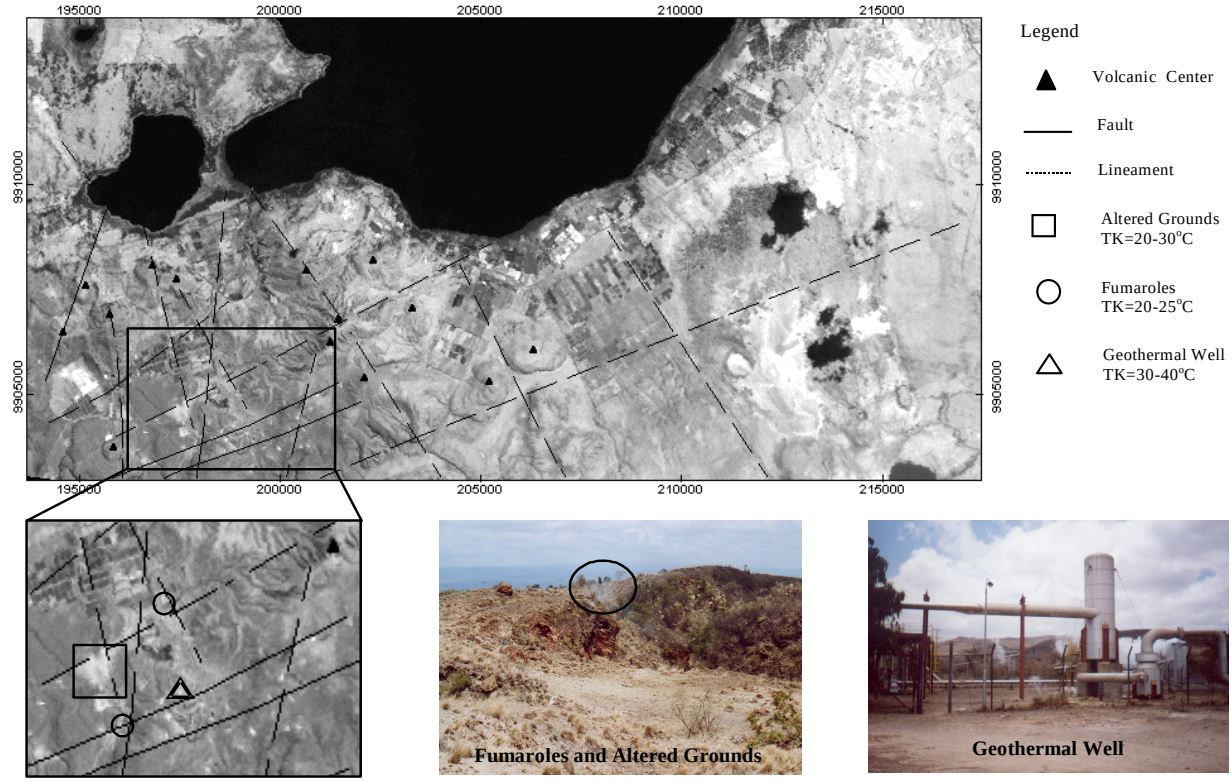


Figure 4: Simplified Geologic Map Lake Naivasha, Kenya (Adapted from Clarke, M. C. G. et. al. 1990)

- The water bodies, agricultural areas, urban structures, water channels, dry rocks and soils, humid areas are clearly seen in the image. The water bodies and agricultural areas in general appear in darker tone compared to the dry rocks and soils, which appear in lighter tone.

- Geothermal manifestations such as fumaroles and altered ground and geothermal wells also show up on the image as scattered points. These features appear to be restricted on the west side of the main thermal divide in a NE-SW direction especially along the Olkaria Fault Zone.

4.2 Quantitative Interpretation

In thermal infrared (IR) sensing, radiation emitted by the ground objects is measured for temperature estimation. The DN values in TM-6 are the most important data for estimating temperature. The radiant temperatures corresponding to all the DN values were determined. Calculations of radiant temperature from DN values have to be through corresponding spectral radiance values. The following equation developed by the National Aeronautics and Space Agency (NASA) (Markham and Barker, 1986) for the Landsat TM-6 can be used for computing spectral radiance:

$$L_{(\lambda)} = L_{\min(\lambda)} + \left[\frac{\left(L_{\max(\lambda)} - L_{\min(\lambda)}\right)}{Q_{cal\max}} \right] \cdot Q_{cal} \quad (1)$$

Where:

$L_{(\lambda)}$ – spectral radiance received by the sensor for the pixel

$L_{\min(\lambda)}$ – minimum detected spectral radiance for the scene (0.1238 $mWcm^{-2}sr^{-1}\mu m^{-1}$)

$L_{\max(\lambda)}$ – maximum detected spectral radiance for the scene (1.56 $mWcm^{-2}sr^{-1}\mu m^{-1}$)

Q_{calmax} – maximum grey level (255)

Q_{cal} – DN value for the pixel

Once the spectral radiance $L_{(\lambda)}$ is computed, it is possible to calculate radiant temperature directly by the following equation:

$$T_R = \frac{K_2}{\ln\left(\frac{K_1}{L_{(\lambda)}} + 1\right)} \quad (2)$$

Where:

T_R - radiant temperature in Kelvin for the pixel in question

K_1 - calibration constant (60.776 $mWcm^{-2}sr^{-1}\mu m^{-1}$)

K_2 - calibration constant(1260.56 K)

$L_{(\lambda)}$ - spectral radiance for the pixel in question, calculated above

From the radiant temperature, kinetic temperature (TK), can be calculated using the equation:

$$T_R = \varepsilon_{\lambda}^{\frac{1}{4}} \cdot T_K \quad (3)$$

Where:

ε_{λ} - spectral emissivity

The DN values from the image for some of the features in the study area were determined using Integrated Land and Water Information System (ILWIS) developed by the International Institute for Aerospace Survey and Earth Sciences (ITC) in the Netherlands. The DN values of the lake range from 9-15 while that of the geothermal manifestations and wells overlaps in a range of 110-140. The volcanic rocks consisting mainly of rhyolite and pyroclastic rocks in the Olkaria Volcanic Complex have DN values ranging from 40-80 while the pyroclastic deposits composed of ashes, tuff and pumic and lava flow predominantly of trachytic composition at the slopes of Mt. Longonot have DN values ranging from 110-130.

The equations above were applied to the raw TM-6 image using ILWIS to come up with a kinetic temperature map in ^{o}C. A uniform spectral emissivity value of 0.95 has been used in the calculation as most of the rock/soil types present in the area have spectral emissivity value close to 0.95.

A density slicing technique was applied in the resulting kinetic temperature map. This is to classify the map into series of intervals corresponding to a specified temperature range. A classified temperature map is shown in Figure 5. It could be observed that geothermal features and wells show up on the surface as high temperature pixels with values ranging from 20-40^{o}C with a background temperature between 0-15^{o}C. The temperatures obtained are not absolute temperature but only relative temperature of the ground surface.

4. CONCLUSION

The thermal manifestations and structural features in general show a relation with high heat flow. Temperature differences in the thermal image can also aid in the description and distribution of various rock types. Based from the above observations, a thermal image appears to have a potential application for geothermal application. With the availability of ASTER (Advanced Spaceborne Thermal Emission and Reflection Radiometer) images, which boasts of a five-band configuration over thermal infrared region and a high resolution, thermal remote sensing for geothermal exploration and other application holds much promise.

4. ACKNOWLEDGEMENT

The paper was part of my study in the International Institute of Aerospace Survey and Earth Sciences (ITC) in the Netherlands in 2001. Thanks to Ms. Anupma Prakash and Rob Sporry for the support and encouragement. Thanks also to the people of Naivasha and KENGEN for the assistance. The Landsat TM Image and other reference materials were provided by (ITC).

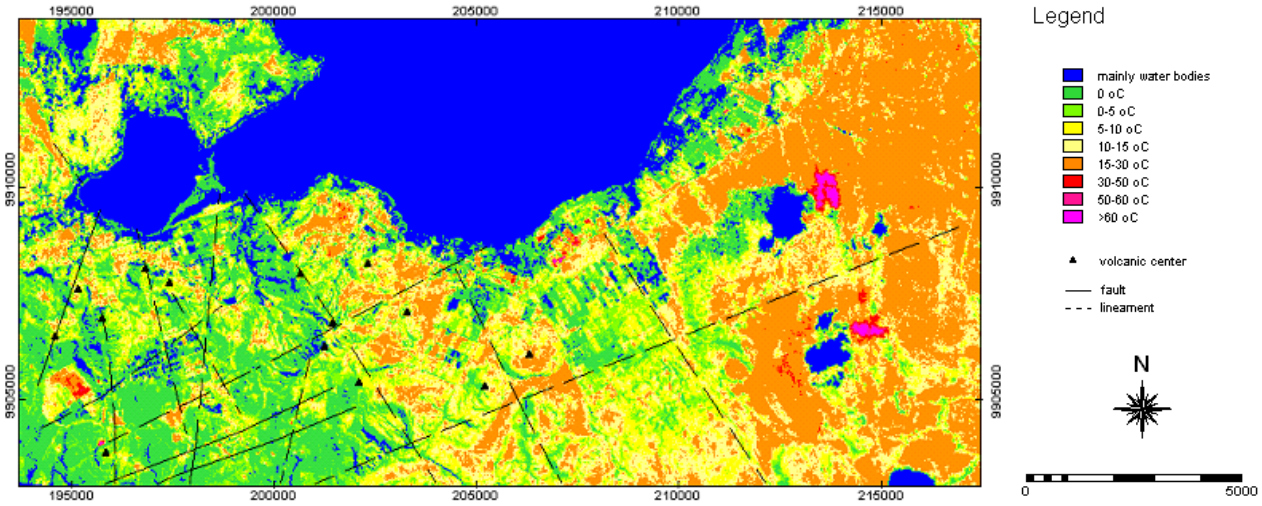


Figure 5. Temperature Map South of Lake Naivasha

REFERENCES

Clarke, M. C. G., D. Goodhall, D. Allen and G. Darling: Geological, Volcanological and Hydrogeological Controls on the Occurrence of Geothermal Activity in the area surrounding Lake Naivasha, Ministry of Energy Report, 138 p., Nairobi, Kenya (1990)

Lillesand, T. M. and R. W. Keefer: Remote Sensing and Image Interpretation. Third Edition. Wiley and Sons, New York (1994)

Markham, B. L. and Barker, J. L.: Landsat-MSS and TM post calibration dynamic ranges, exoatmosperic reflectances and at-satellites temperatures. EOSAT Landsat Technical Notes 1. pp. 3-8. Lanham, Maryland: Earth Observation Satellite Company (1986)

Omenda, P. A.: The Geology and Structural Controls of the Olkaria Geothermal System, Kenya. *Geothermics*, Vol. 27, No. 1, pp. 55-74 (1999)

Pastor, M. S.: Geophysical Study of Groundwater System south of Lake Naivasha. M. Sc. Thesis, International Institute for Aerospace Survey and Earth Sciences (ITC), Netherlands (2001)

Sabins, F. F.: Remote Sensing: Principles and Interpretation, Third Edition (1996)

Saraf, A. K, A. Prakash, S. Sengupta and R. P. Gupta: Landsat TM data for Estimating Ground Temperature and Depth of Subsurface Coal Fires in the Jharia Coalfield, India. International Journal of Remote Sensing, Volume 16, No. 12, 2111-2124 (1995)